eTransportation 24 (2025) 100394

Contents lists available at ScienceDirect

eTransportation

journal homepage: www.journals.elsevier.com/etransportation

Centralised vehicle-to-grid smart charging supported by PV generation for power variance minimisation at the transformer: A user's perspective analysis

M. Secchi [a,*], D. Macii [b], G. Barchi [c], M. Marinelli [a]

[a] Technical University of Denmark, Department of Wind and Energy Systems, Anker Engelunds Vej 1, Kgs. Lyngby, 2800, Denmark
[b] University of Trento, Department of Industrial Engineering, Via Sommarive 9, Trento, 38123, Italy
[c] EURAC Research, Institute for Renewable Energy, Viale Druso/Drususallee, 1, Bolzano/Bozen, 39100, Italy

ARTICLE INFO

Keywords:
Vehicle-to-grid (V2G)
Smart EV charging
Photovoltaic production (PV)
EV battery degradation
Quadratically-constrained quadratic programming

ABSTRACT

Recent studies show that the electric vehicle (EV) fleet in the EU will reach 37–38 million units by 2035. Most of them are expected to be charged at home, boosting the number of residential charging stations to be installed. In order to decrease their environmental impact, these stations should be powered by clean energy sources, such as distributed photovoltaic (PV) generators. However, the increased penetration of EVs and PVs may cause large power supply and demand fluctuations, stressing the substation transformers. This paper proposes a centralised bidirectional Vehicle-to-Grid (V2G) smart EV charging policy minimising the net-load power variance (NLV) at the transformer. The proposed approach relies on the iterative solution of a Mixed-Integer Quadratically-Constrained Quadratic Programming (MIQCQP) problem that, unlike other research papers, keeps into account users' charging/discharging requirements, and realistic charging limitations and efficiency. The impact of the resulting EV charging schedules is analysed at a district level for growing EV and PV penetration values, then compared with the results obtained with both unidirectional (V1G) and uncontrolled (UC) EV charging. Key elements of novelty of the work are: (i) the formalisation of the optimisation problem and its scalability potential, allowing for a multi-year analysis; (ii) an accurate assessment of the user self-sufficiency and the EV battery degradation by means of a physics-inspired model; (iii) an evaluation of the potential economic impact for EV owners over multiple years. Applying the proposed V2G strategy to battery electric vehicles (BEVs) reduces the NLV at the transformer by up to 80%, while increasing self-sufficiency by up to 23%, producing a minimal battery degradation. In the current market scenario, if the Distribution System Operator (DSO) offers a fair compensation for the V2G grid support, the potential yearly economic savings for battery electric vehicle (BEV) owners equipped with a residential PV generator range between 10% and 20%. This happens despite the higher V2G charging stations' upfront costs and the faster BEV battery degradation.

1. Introduction

In 2021, the EU issued the "Fit for 55" package, elaborating new ambitious scenarios for the European energy transition. One of the most relevant targets concerns the CO_2 emissions from newly sold vehicles and prescribes a 100% reduction by 2035,[1] a target which forces the conversion of old internal combustion engine vehicles (ICVs) to EVs. As a consequence, recent studies show that 37–66 million EVs should circulate by 2030 [1] which would require around 1.4–2.5 million public charging stations [2], without accounting for domestic ones (each EV owner will probably have one at home). The integration of such a large number of chargers at the distribution level poses a threat to the grid stability, due to time-varying generation/load mismatch, increased lines congestion, and load imbalances [3]. However, statistics show that EVs are parked on average for 96% of their lifetime [4]. Thus, suitable smart EV charging techniques can be used to mitigate the impact of EV charging on the power grid. The EVs could also be beneficial to increase the grid capacity to "host" local generation and to mitigate the risk of over-voltage, lines congestion, phase unbalance, and reverse power flows caused by distributed energy resources [5,6]. The so-called "smart chargers", based either on a V1G (unidirectional) or bidirectional (V2G) control, allow users to not only delay the charging session start and down-modulate its power, but also to discharge their batteries at peak loading times. Using EV batteries as additional mobile storage systems, in addition to the stationary ones, may actively

* Corresponding author.
E-mail addresses: matsec@dtu.dk (M. Secchi), david.macii@unitn.it (D. Macii), grazia.barchi@eurac.edu (G. Barchi), matm@dtu.dk (M. Marinelli).

[1] Directive 2014/94/EU on the Alternative Fuels Infrastructure (AFID) https://eur-lex.europa.eu/legal-content/en/TXT/?uri=CELEX:52021PC0559

https://doi.org/10.1016/j.etran.2025.100394
Received 14 March 2024; Received in revised form 10 January 2025; Accepted 13 January 2025
Available online 24 January 2025

Nomenclature

ΔC^{CAL}	Capacity decrease due to calendar battery ageing.
ΔC^{CYC}	Capacity decrease due to cycling battery ageing.
ΔSOH	Variation in the EV battery State-of-health during its lifetime.
Δt	Simulation timestep length in hours.
η	EV on-board charger charging/discharging efficiency.
$\mathcal{T}$	Set of the T time instants in a day.
$\mathcal{T}_s$	Subset of $\mathcal{T}$ collecting the instants of the sth charging session.
$\mathcal{U}$	Set of the M households connected to the network.
$\mathcal{U}_{EV}$	Subset of $\mathcal{U}$ including the N EV owners.
$\mathcal{U}_{PV}$	Subset of $\mathcal{U}$ including the K PV system owners.
ρ	Charging/discharging rate of the EV battery.
τ	Index of the charging instants in subset $\mathcal{T}_s$.
B	Arbitrarily big number used to formalise the optimisation problem.
C	EV battery capacity size.
c^{buy}	Retail price of electricity including system charges and taxes.
c^{deg}	Yearly cost due to battery degradation.
c^{hw}	Yearly cost for purchasing and maintaining the EV charger.
c^{sell}	Electricity selling price, a.k.a. hourly day-ahead market price.
CF	Yearly cash flow including degradation and hardware purchase/maintenance costs.
CF^*	CF plus a compensation for the energy stored in the EVs and sold to the system at a later time.
E_a	Activation energy of the battery chemical reaction.
EV_{share}	Share of the M households with an EV charging station.
f	Pre-exponential factor for battery degradation.
I	Instantaneous current flowing to/from the EV battery.
i	Index for the households.
j	Index for the EV owners.
K	Number of households/users equipped with a PV system.
LT_{EV}	Predicted EV lifetime.
M	Number of households/users connected to the network.
N	Number of EV charging stations (and EVs).
$NLVR$	Net Load Variance Reduction.
P	Active power mismatch at the secondary substation transformer.
p^{EV}	Instantaneous power absorbed by the EV charging station.
p^{L}	Instantaneous power absorbed by domestic appliances.
P^{max}	Maximum power absorbed by an EV.
P^{min}	Minimum power absorbed by an EV.
p^{NET}	Instantaneous net power measured by the domestic smart meter.
p^{PV}	Instantaneous power produced by the PV system.
PV_{share}	Share of the M households with a PV system.
R	Universal gas constant.
S	Number of charging sessions during the day.
s	Index for the EV charging session.
SOC^e	EV "departure" state-of-charge at the end of the charging session.
SOC^i	EV "arrival" state-of-charge at the beginning of the charging session.
SOC^{max}	Maximum attainable state-of-charge of the EV battery.
SOC^{min}	Minimum attainable state-of-charge of the EV battery.
SU	Self Sufficiency, i.e. the share of the appliances and EV load covered by PV.
T	Number of time instants in a day (96).
t	Index for the simulation time instant.
t^e	Charging session ending index.
t^i	Charging session starting index.
T_b	EV battery pack temperature.
Y	Number of Δt-long timesteps in a year.
y	Binary variable representing charging (0) or discharging (1).

contribute to peak-shaving and shifting the load [7].

In this paper, we propose and analyse the impact of a centralised coordinated V2G-based smart EV charging scheme from the users' perspective. Such a smart charging (SC) policy is designed to level out the overall active power fluctuations at the Medium-Voltage/Low-Voltage (MV/LV) transformer of a district substation. The rest of the paper is structured as follows. In Section 2, the most relevant pieces of literature about this topic are presented to better contextualise our contribution. In Section 3, the chosen smart EV charging policy is both quantitatively described and mathematically formalised as an optimisation problem. Section 4 describes the chosen case study, the related simulation settings, and reports the results of the smart EV charging algorithm chosen to solve the optimisation problem. Section 5 shows the impact of smart EV charging on district-level self-sufficiency (along with the related CO2 emissions), EV battery degradation, and the possible economic savings for EV owners. Finally, Section 6 concludes the paper and outlines the future work.

2. Related work

Many studies tackled the problem of scheduling the charging of EVs to attain some particular objective. The approaches found in the literature can generally be classified as "centralised" or "decentralised", the difference being whether the EVs are controlled centrally by an aggregator or not. Some relevant papers on centralised smart EV charging are listed in Table 1.

Among them, various scheduling objectives are chosen. Net-load balancing, peak-shaving, valley-filling, and net-load variance minimisation are all cases where the EVs are used to mitigate the power fluctuations over the grid due to time-varying load or generation patterns.

Table 1
Relevant literature overview on centralised smart EV charging techniques for net-load levelling. GA=Genetic Algorithm, PSO=Particle Swarm Optimisation, QP=Quadratic Programming, LP=Linear Programming, MI=Mixed-Integer, ML=Machine Learning, MC=Monte-Carlo, RBC=Rule-Based Control, NLP=Non-Linear Programming.

Objective	Methodology	User Benefit Analysis	Realistic EV Charging Constraints	Battery Degradation	Impact of DERs	Examples
Minimising NLV	GA	No	No	No	Yes	[14]
	QP	No	No	No	Yes	[20]
		No	No	Yes	Yes	[7]
	MIQCQP	**Yes**	**Yes**	**Yes**	**Yes**	**This Paper**
Net-Load Balancing	PSO	No	No	No	Yes	[12]
	PSO	No	No	No	Yes	[12]
	LP	Yes	No	No	Yes	[18]
		Yes	No	No	Yes	[19]
	NLP	Yes	No	No	Yes	[26]
		Yes	No	No	Yes	[27]
	QP	No	No	No	Yes	[21,22]
Peak-Shaving + Valley-Filling	MINLP	Yes	No	No	No	[25]
	MIQP	No	No	Yes	No	[23]
	MILP	Yes	No	Yes	Yes	[24]
	PSO	No	No	Yes	Yes	[13]
		Yes	No	Yes	No	[11]
	ML	Yes	No	Yes	No	[15]
		No	No	Yes	Yes	[16]
		Yes	No	No	No	[17]
	RBC	Yes	No	No	No	[8]
		No	No	No	Yes	[9]
	RBC+GA	No	No	No	No	[10]

Besides a different formalisation, different scheduling and optimisation techniques are used, depending on the linear or non-linear nature of the objective function and the related constraints. For example, in [8–10], rule-based controls are used, while in [11–13], Particle Swarm Optimisation (PSO) is applied. The use of genetic algorithms (GAs) is also common (e.g., in [14]). Recently, several machine learning (ML) techniques have been widely adopted [15–17]. Linear programming (LP) is used in [18,19], while quadratic programming (QP) is chosen in [7,20–22]. Sometimes mixed-integer quadratic (MIQP) [23], linear (MILP) [24] or non-linear (NLP) [25–27] programming techniques are deployed.

In this paper, we aim to expand the work done in the field of smart EV charging by formalising and solving a scalable Mixed-Integer Quadratically-Constrained Quadratic Programming (MIQCQP) problem. Similarly to other approaches, the main goal is to optimise the daily charging schedule of the EVs within a given district according to a V2G approach.

However, our approach keeps into account both the charging/discharging efficiencies and the minimum/maximum charging power levels, which may greatly affect the smart charging effectiveness but are mostly overlooked in other research works.

Moreover, the algorithm is very flexible, as it can exclude some EVs from grid support (i.e., it can turn the V2G charging mode of some EVs into V1G mode) by simply changing some constraints, which also simplifies the problem solution. This is useful for instance in the case of plug-in hybrid EVs, whose battery capacity is too small to support the grid. Additionally, the algorithm chosen to solve the MIPCQP problem mitigates the large memory and processing power requirements of other monolithic quadratic programming optimisation techniques through an iterative approach. This methodology returns a sequence of locally optimal EV charging schedules that greatly improve the scalability of the V2G smart charging policy. As a result, we could perform a thorough analysis of the impact of smart EV charging over one year, considering increasing penetration levels of PV systems and EVs, and including both the battery degradation effects and the benefits of a possible compensation for the EV owners that participate in the service. It is worth emphasising that, to the best of Authors' knowledge, the battery degradation issue was considered in [7,23,24] only, but it was not studied using an accurate physics-inspired model. Finally, none of the works presented in Table 1 provides such an extensive and multifaceted analysis of the impact of a V2G charging strategy on EV users.

3. Smart EV charging algorithm

In this Section, the smart EV charging approach is described in detail. A qualitative overview of the overall architecture including the main control signals is shown in Fig. 1. The proposed approach is centralised, in line with other solutions proposed in the technical literature [22,28]. In this type of solution, a central aggregator is supposed to collect data from EV owners, including:

- the start and end time of each EV charging session, as well as its duration;
- the initial and expected final State of Charge (SOC) values for each session;
- the nominal and effective capacity of each EV's battery;
- the minimum and maximum charging and discharging power of each charging station.

Moreover, the DSO is supposed to provide the aggregator with the total aggregated net-load power at the transformer. The aggregator then uses the aforementioned data collected over a given time interval (e.g., one day split into slots of 15 min each), to solve an optimisation problem that returns: (i) a sequence of binary values (depending on whether an EV is actually under charge, or it instead injects power to the grid in a given time slot); and (ii) the corresponding positive or negative power levels for the various charging stations. The goal of the optimisation problem implemented and solved by the aggregator is to minimise the total net-load variance (NLV) of the active power profile at the MV/LV substation transformer, while keeping into account both charging/discharging constraints and users' needs. The optimisation problem is formalised in Section 3.1, and further implementation details and a discussion on its computational complexity are reported in Section 3.2.

3.1. Optimisation problem formulation

Let us consider a district with M users gathered in a set called $\mathcal{U}$. Let $\mathcal{U}_{PV}$ and $\mathcal{U}_{EV}$ be the sets including the $K \leq M$ users and the $N \leq M$ users equipped with a PV system or with an EV charging station, respectively. It is worth noticing that these subsets generally do not coincide. We can thus define the share of users equipped with a PV system or with a charging station as $PV_{share} = \frac{K}{M} < 100\%$ and $EV_{share} = \frac{N}{M} < 100\%$, respectively. In the following, we will assume, for the sake of simplicity, that each EV is charged only by its residential

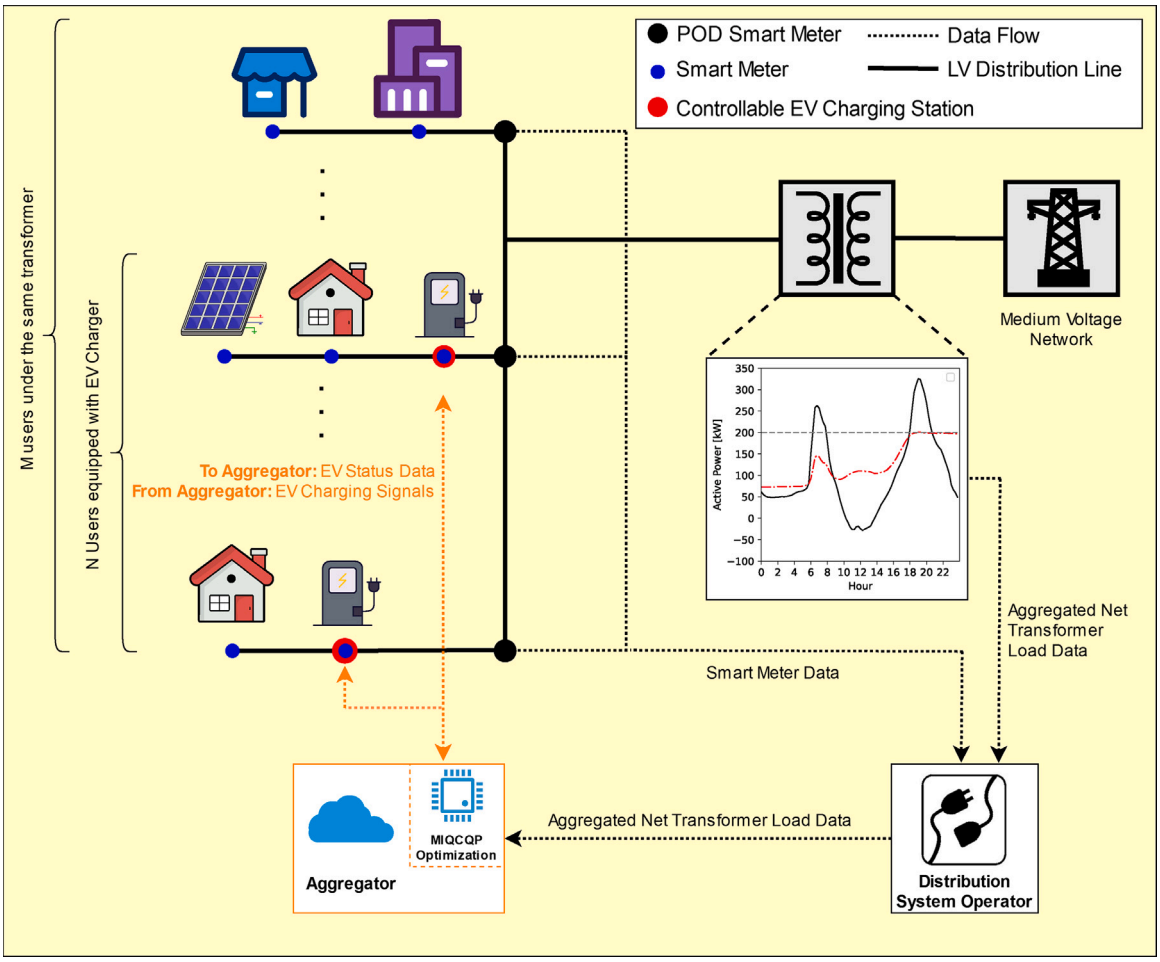

Fig. 1. Overview of the architecture of the proposed centralised V2G-based smart EV charging approach along with the main signals controlling the process.

charging station.

The symbols needed to formalise the smart EV charging problem are listed in the preliminary nomenclature Section, but they are also described in greater detail in the following, for the sake of clarity.

- Index $j \in \mathcal{U}_{EV}$ refers to the j−th EV extracted from the set of available EVs to schedule its daily charging/discharging pattern. Since $N!$ permutations of N distinct values exist, if $\alpha(\cdot)$ denotes any bijective permutation function of the elements of $\mathcal{U}_{EV}$, for each index $n = 0, \dots, N$, then $j = \alpha(n)$ denotes the index of the j−th EV that is selected for smart charging. Therefore, the sequence of j values establishes the order in which the optimal EV charging schedule is performed during the n−th iteration of the algorithm;
- $t \in \mathcal{T} = \{1, \dots, T\}$ is the index of the t−th time slot of duration Δt in the period over which the optimisation problem is solved;
- S_j is the number of times the j−th EV is actually connected to the charging station within $\mathcal{T}$;
- $\mathcal{T}_{s_j} = \{t^i_{s,j}, \dots, t^i_{s,j}\} \subseteq \mathcal{T}$ is the subset of time slots of the s−th charging session of the j−th EV. Each charging session starts at time $t^i_{s,j}$ and ends at time $t^e_{s,j}$ for $s = 1, \dots, S_j$;
- $SOC^i_{s_j}$ and $SOC^e_{s_j}$ are the SOC values of the EV battery at the beginning and at the end of the s−th charging session;
- $SOC^{\min}$ and $SOC^{\max}$ are the minimum and SOC levels that should never be exceeded to avoid excessive battery degradation and keep a minimum "emergency" energy content in the battery, respectively.
- Parameters C_j and η_j denote the battery capacity of the jth vehicle and the corresponding typical power conversion efficiency. For the sake of simplicity, and with no loss of generality, in the following, the typical charging and discharging efficiency are assumed to be equal.
- $P^{\min}$ and $P^{\max}$ are the minimum and maximum allowed power values for EV charging and discharging due to technology, safety, or contractual limitations. Again, with no loss of generality, such values in the following will be assumed to be the same for all EVs and charging stations.
- Finally, for each EV $j \in \mathcal{U}_{EV}$, the corresponding set of decision variables of the considered optimisation problem can be enclosed into vector $\mathbf{x}_j = [p^{EV}_{j,1}, \dots, p^{EV}_{j,T}, y_{j,1}, \dots, y_{j,T}]^T$, where $p^{EV}_{j,t}$ is the amount of average power drawn from (or injected into) the battery in each time slot $t \in \bigcup \mathcal{T}_{s_j}$, and $y_{j,t}$ is a binary variable equalling 1 if the EV battery is discharged, or 0 if the EV is charged.

Based on the notation above, assuming to schedule the charging/discharging of one EV at a time (further details motivating this choice are reported in Section 3.2), the total power at the substation in each time slot $t \in \mathcal{T}$ can be recursively expressed as

$$P_{t_n} = P_{t_{n-1}} + \begin{cases} p^{EV}_{j,t} & t \in \bigcup \mathcal{T}_{s_j} \\ 0 & t \notin \bigcup \mathcal{T}_{s_j} \end{cases} \quad j = \alpha(n) \quad n = 0, \dots, N \tag{1}$$

where $P_{t_0} = P^{Base}_t = \sum_{i \in \mathcal{U}} p^L_{i,t} - \sum_{k \in \mathcal{U}_{PV}} p^{PV}_{k,t}$ is the baseline average net-load power at the substation within the t−th time slot at iteration $n = 0$, i.e., when no EV charging has been scheduled yet. Note that P^{Base}_t is given by the difference between the total power demand of all users in time slot t ($p^L_{i,t}, \forall i \in \mathcal{U}$) and the aggregated power generated by the distributed PV systems in the same time slot (i.e., $p^{PV}_{k,t}, \forall k \in \mathcal{U}_{PV}$).

By applying (1), a possible smart charging schedule of all EVs results from the iterative minimisation of the total net load variance at the substation, as the number of EVs increases. Thus, the following optimisation problem must be solved N times (i.e., for $n = 1, \dots, N$):

$$\mathbf{x}_j = \operatorname{argmin}\left[\widehat{\operatorname{var}}(P_n)\right] = \operatorname{argmin}\left[\frac{1}{T}\sum_{t=1}^{T}\left(P_{t_n} - \frac{1}{T}\sum_{t=1}^{T}P_{t_n}\right)^2\right] \quad \text{for } j = \alpha(n) \tag{2}$$

where $\widehat{\operatorname{var}}(\cdot)$ denotes the variance estimator of the random variable chosen as argument. Note that, in the following, t_n will be simplified as t for the sake of brevity.

The constraints of the optimisation problem are summarised below.

i. **EV charging requirements**: the EV battery can be charged or discharged only when the vehicle is connected to the grid. While the initial SOC of the battery at connection time depends on the previous use of the vehicle, the final SOC (i.e., at disconnection time) must meet the user's expectations (usually SOC^{max}=90%). Therefore, the $p_{j,t}^{EV}$ profile during the $s-$th charging session of vehicle j should not violate the usage requirements of a given user. Thus, with reference to the notation listed above, the following quadratic equality constraints must be included in the optimisation problem, i.e.

$$\sum_{t\in\mathcal{T}_{s_j}} \frac{p_{j,t}^{EV}}{C_j}\left[(1-y_{j,t})\eta_j + \frac{y_{j,t}}{\eta_j}\right]\Delta t = (SOC_{s_j}^{e} - SOC_{s_j}^{i})$$
$$s = 1, \dots, S_j, \quad j = \alpha(n) \tag{3}$$

Note that, when $y_{j,t} = 0$ (EV battery charging), the amount of energy injected into the battery of the $j-$th EV is lower than expected due to the limited efficiency factor η_j, whereas when $y_{j,t} = 1$ (EV battery discharging), for a given amount of power injected into the grid, the corresponding SOC reduction is divided by η_j, to keep into account the losses due to the finite efficiency of battery discharging.

ii. **No excessive EV battery charging and discharging**: as known, excessive battery charging reduces the battery lifetime [29,30], while discharging may lead to EV usability issues, e.g., the EV owner needs the car but not enough energy is available. To mitigate these problems, during each charging session, the SOC should never exceed $SOC^{\max}$ nor fall below $SOC^{\min}$. As a consequence, the following additional quadratic inequality constraints have to be considered, i.e.

$$SOC^{\min} \le SOC_{s_j}^{i} + \sum_{\tau} \frac{p_{j,t}^{EV}}{C_j}\left[(1-y_{j,t})\eta_j + \frac{y_{j,t}}{\eta_j}\right]\Delta t \le SOC^{\max}$$
$$\forall \tau \in \mathcal{T}_{s_j}, \quad s = 1, \dots, S_j, \quad j = \alpha(n) \tag{4}$$

iii. **Maximum/minimum charging and discharging power**: This final set of inequality constraints to be included in the optimisation problem, can be easily expressed as

$$P^{\min} \le |p_{j,t}^{EV}| \le P^{\max}$$
$$\forall t \in \mathcal{T}_{s_j}, \quad s = 1, \dots, S_j, \quad j = \alpha(n) \tag{5}$$

where $P^{\min}$ is the minimum "activation" charging/discharging power according to the IEC Standard 61851 [31], while $P^{\max}$ is the maximum allowed charging/discharging power due to the charging station capabilities, the supply contract, or the EV battery management system. While the formulation of (5) is rather simple, its implementation is complicated by the fact that the feasibility region associated with the leftmost inequality is non-convex. This problem can be solved by relying on the same binary decision values already used to discriminate the time slots when an EV is charged and discharged. Indeed, as explained in [32], (5) can be transformed into

$$\begin{cases} |p_{j,t}^{EV}| \le P^{\max} \\ p_{j,t}^{EV} + B y_{j,t} \ge P^{\min} \\ p_{j,t}^{EV} - B(1-y_{j,t}) \le -P^{\min} \end{cases}$$
$$\forall \tau \in \mathcal{T}_{s_j}, \quad s = 1, \dots, S_j, \quad j = \alpha(n) \tag{6}$$

where B is a constant value that must be set large enough to ensure that either the second or the third constraint is always met for some values of $y_{j,t}$. Indeed, when $y_{j,t} = 0$, the second constraint limits the minimum charging power to be $p_{j,t}^{EV} \ge P^{\min}$, while the third one is always satisfied. Conversely, when $y_{j,t} = 1$ (discharging), the second constraint is always satisfied, and the third one limits the minimum discharging power to be $p_{j,t}^{EV} \le -P^{\min}$.

Some additional notes on the optimisation problem based on expressions (2)–(6) are summarised below.

- Even if the EV charging/discharging profile changes as a function of $\alpha(\cdot)$ (namely on the order in which EVs are virtually selected/extracted from the set of district vehicles), several Monte Carlo simulations for the case study described in Section 4 (not reported here for the sake of brevity) confirmed that the actual impact of the sequence of j values on the analysis described in Section 5 is negligible.
- The proposed approach can be applied whenever the central coordinator is able to forecast the EVs' arrival time and the connection duration with adequate accuracy. Forecasting can be based on historical data and/or on some ad-hoc algorithm. If an EV owner accepts the proposed schedule, the coordinator updates the baseline load conditions accordingly, and the smart charging schedule of the following EV is computed based on the updated information.

3.2. Computational complexity analysis

The smart EV charging problem formulated in Section 3.1 is inherently different from other similar problems aimed at minimising the NLV. Indeed, most of them can be regarded as standard convex QP problems [7,20–22]. Therefore, they can be solved in a polynomial time. Indeed, the most known algorithms solving such problems (e.g., the interior point method) have a worst-case complexity of around $O(n^3)$ that can be reduced further when sparse problems are considered. If the number of variables is large, significant computational benefits can be obtained by using genetic algorithms, although at the price of slightly suboptimal solutions [20].

In this paper, even if the NLV function (2) is the same as in other QP problems [7,22], the linear or quadratic constraints (3), (4) and (6), depend on the integer (i.e., binary) variables $y_{i,t}$ that denote if, in each time slot of a charging session, the EV battery is really under charge or it is rather discharged. As a result, the optimisation problem formalised in Section 3.1 is an MIQCQP one that, unfortunately, is NP-hard [33]. This explains why a greedy iterative approach is the most sensible way to find reasonable, although suboptimal, solutions while ensuring scalability. Indeed, by computing the optimal charging/discharging schedule of just one EV at a time, the monolithic MIQCQP problem involving all EVs can be decomposed into a sequence of smaller MIQCQP problems whose number of variables (as well as the related memory and computation requirements) is kept bounded by the limited duration of the charging sessions, that in turn is typically much lower than T. At each iteration, the local optimal solution can be found by using standard optimisation tools within a branch-and-bound framework. First, the convexity of the objective function is exploited to

solve a continuous relaxation of the problem, thus efficiently finding a lower bound. It then systematically explores branches by fixing binary variables to 0 or 1, solving relaxations at each step. Cutting planes (like Gomory or mixed integer rounding cuts) are used to tighten the relaxation and reduce the search space. The convexity of the objective function ensures that a local optimal solution can be found efficiently in each iteration.

With the adopted iterative approach, the computational burden grows just linearly with the number of EVs, thus enabling long-term performance and impact analyses when the number of EVs grows significantly, as it will be shown in Section 5.

4. Case study description and optimisation results

In this section, we describe how the baseline load, the PV power profiles, and the EV charging profiles were generated. Moreover, the main simulation parameters, settings, and simulated scenarios are listed.

4.1. Baseline load profiles

The study considers a district with $M = 297$ households. The house load profiles were created through the Load Profile Generator[2] software. The simulated buildings include both single-family (detached) houses, and buildings composed of four to six flats.

4.2. EV load profiles

The EV charging sessions parameters, i.e. their length, starting time, and nominal charging power, were generated with the RAMP-mobility[3] software, a stochastic EV charging profiles generator. The main parameters of the EVs used in the simulations are listed below:

- **Battery Size:** $C_j = 10 - 14$ kWh for Plug-in Hybrid Electric Vehicles (PHEVs) and $37 - 100$ kWh for Battery Electric Vehicles (BEVs), as reported by the Italian authority for the electricity market regulation.[4]
- **EV Type Share:** 58% of the fleet consists of PHEVs, whereas the remaining 42% are BEVs, as reported in a recent Italian market analysis.[5] This also in agreement with the electrical mobility scenarios reported by the Italian Transmission System Operator (TSO).[6]
- **Min. Charging Power:** $P^{\min}$ is set to 1.38 kW (6 A, single phase, 230 V) in accordance with the IEC Standard 61851 [31]. Indeed, the EVs charging/discharging currents should never be lower than 6 A, otherwise the charging/discharging efficiency drops well below 50%, as shown in Fig. 2.
- **Max. Charging Power:** Assuming that single-phase charging stations operating at 230 VRMS and 32 A are used, $P^{\max}$ is set to 7.4 kW. This power level provides a good trade-off between the most common current scenario (most of the currently circulating PHEVs and BEVs can charge at 3.7 kW), and the future one (most BEVs can already charge at 11–22 kW). Moreover, most of the currently available EVs (including the PHEVs) can be charged at 7.4 kW [34]. Thus, when (5) is applied, the sequence of $p_{j,t}^{EV}$ values lie in the intervals $[-7.4\ \text{kW}, -1.38\ \text{kW}] \vee [1.38\ \text{kW}, 7.4\ \text{kW}]$.
- **EV Charging/Discharging Efficiency:** The real-world EV charging/discharging efficiency highly depends on (i) the power level, (ii) the number of phases used, (iii) the AC/DC and DC/AC power converters, (iv) the battery SOC. However, we could not assume that the efficiency changes as a function of the actual charging or discharging power, otherwise the smart EV charging optimisation problem would become nonlinear and therefore much more computationally demanding. To bypass this problem, a threshold approach was used, i.e., the values of η_j in (3) and (4) were assumed to be constant within $[-7.4\ \text{kW}, -1.38\ \text{kW}] \vee [1.38\ \text{kW}, 7.4\ \text{kW}]$. In particular, the efficiency was assumed to be equal to 82%, which is indeed within the efficiency range associated with the chosen charging/discharging power intervals, and it is also in line with other values reported in the technical literature [35].
- **Maximum and minimum SOC:** $SOC^{\max}$=90% to avoid excessive battery wear [36], and $SOC^{\min}$=20% to have an "emergency" battery energy level.

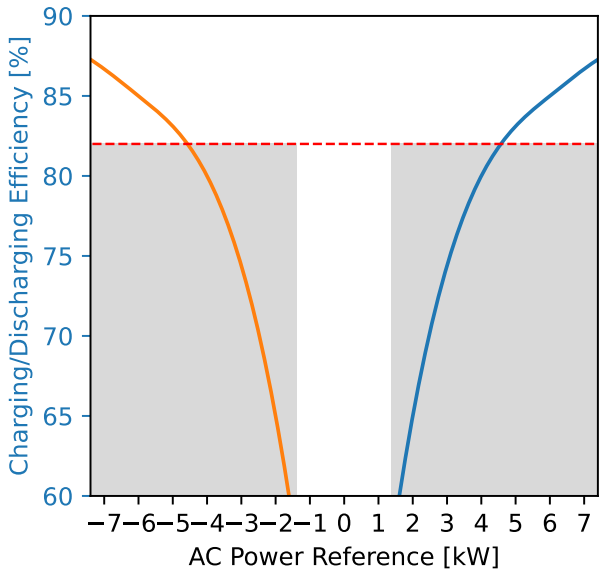

Fig. 2. Example of efficiency curves as a function of charging/discharging power, as presented in [37].

The total yearly energy consumption of a BEV in Italy is about 2.05 MWh on average, which corresponds to about 30 km/day per EV (around 11500 km/year) as reported by car manufacturers. Note that the battery capacity not only of the BEVs (37–100 kWh) but also of the PHEVs (10–14 kWh), is large enough to cover the typical range of a daily commute, i.e. between 35 km and 50 km. The charging sessions mostly start in the early evening during weekdays, while they occur throughout the day at the weekends. All of the EV charging profiles generated by RAMP-mobility do not depend on the grid status. Hence, when an EV is connected, the maximum amount of power is drawn from each charging station until the target SOC (usually the maximum allowed) is reached. The resulting "Uncontrolled" (UC) charging profiles will be considered as the baseline to test the efficiency of the smart EV charging algorithm.

4.3. PV generation profiles

Without loss of generality, the irradiation and external air temperature profiles (measured in Bolzano/Bozen, Italy in 2019) are assumed to

[2] LPG: A Bottom-Up Customisable Load Generator, Noah Pflugradt, https://www.loadprofilegenerator.de

[3] RAMP-mobility: a RAMP application for generating bottom-up stochastic electric vehicles load profile https://github.com/RAMP-project/RAMP-mobility

[4] ARERA's Consultation Document 449/2022 for Electric Mobility Scenarios in Italy, https://www.arera.it/fileadmin/allegati/docs/22/449-22.pdf

[5] Motus-E Market Analysis, https://www.motus-e.org/analisi-di-mercato/gennaio-2022-i-primi-segnali-dellassenza-di-incentivi

[6] Terna-SNAM: Electro-mobility Scenarios Description Document, https://download.terna.it/terna/Documento_Descrizione_Scenari_2022_8da74044f6ee28d.pdf

be the same for all households. The installed PV capacity is sized so that each PV system produces the same amount of energy that is consumed over one year [38]. Thus, the installed PV capacity per household ranges between 1.5 kW and 4 kW, with a PV panel minimum size of 450 W.

4.4. Simulation settings

The main simulation settings are summarised below.

- **EV/PV penetration levels:** The EV_{share} and PV_{share} values range between 10%–100% and 0%–100%, respectively. A user that is assumed to be equipped with a PV system or an EV charging station, retains them as the values of EV_{share} and PV_{share} increase.
- **V1G and V2G charging policies:** both the V1G and V2G scenarios are analysed. In the first one, the EVs are not allowed to discharge their batteries to support the power grid. To compute the optimal V1G smart charging schedule in the same conditions as in the V2G case, $y_{j,t} = 0$ for $\forall j \in \mathcal{U}_{EV}$ and $t \in \mathcal{T}$. In the V2G case instead, with a slight abuse of notation but no loss of generality, the PHEVs are excluded, so the subset of decision variables $y_{j,t}$ for $j \in \mathcal{U}_{EV}$ associated with the PHEVs are all set identically to 0 for $t \in \mathcal{T}$. This choice was made because the degradation analysis showed that frequent charging/discharging of small batteries would excessively degrade their capacity over time, thus making the use of an intensive V2G policy impractical for this kind of EVs.
- **Simulation time step:** The optimisation is performed daily, considering 15-minute-long time slots, in line with the capabilities of recent smart meters [39]. As a consequence, $\Delta t = 900$ s and $T = 96$ time slots per day. These time settings also provide a good trade-off between computational complexity and temporal resolution [40].
- **Time horizon:** for every pair of (PV_{share}, EV_{share}) values, the optimisation is repeated day-by-day over one year, while extrapolating the economic analysis over multiple years, since the battery capacity degrades in a longer period (see Section 5.3).

4.5. Optimal smart EV charging schedule

The performance of the proposed smart EV charging algorithm is hereafter analysed. The MIQCQP optimisation problem described in Section 3 was implemented in Matlab R2023a, and solved by using the GUROBI tool.[7] GUROBI not only relies on a flexible branch-and-bound framework, as explained in Section 3.2, but also applies presolving routines to simplify the problem, and heuristics to quickly find feasible solutions. The simulations were performed using the DTU High-Performance Computing (HPC) Cluster [41], where up to 600 cores are available for scientific computing. Fig. 3 shows an example of the daily active power profile at the substation when both PV_{share} and EV_{share} are equal to 50%.

Different line styles refer to different scenarios, i.e., when no EVs are considered, when the EVs are charged in UC mode, when V1G is used, and finally with the proposed V2G approach. The smoothed power profile obtained with the V2G strategy is almost flat in this example, which confirms the potential effectiveness of our method. A deeper performance analysis for different values of EV_{share} and PV_{share} is shown in Fig. 4, where the variance reduction of the power flow fluctuations at the substation is shown w.r.t. the baseline variance without smart EV charging (net-load variance reduction — NLVR).

[7] GUROBI 10.0.2 for Matlab, https://www.gurobi.com/solutions/gurobi-optimizer/

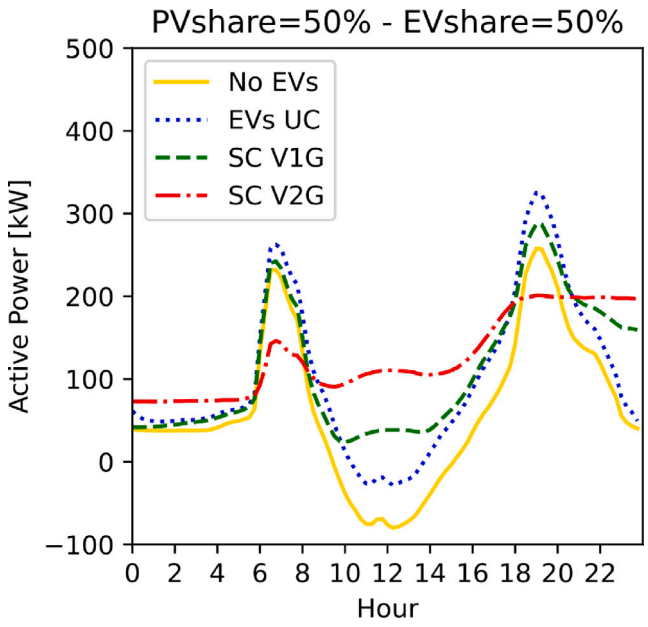

Fig. 3. Example of an aggregated average daily net active power profiles at the substation without EVs and when different EV charging strategies are adopted.

The NLVR contour lines in the plots on the left and on the right of Fig. 4 are obtained respectively when either the V1G or the proposed V2G optimal EV charging strategy are adopted. The NLVR clearly increases with the EV_{share} values, since more EVs can store the PV power over-production. The peak values are, however, different in the V1G and V2G cases. In the former, the maximum NLVR value is about 43%, while in the latter it reaches 81%, due to the massive grid support offered by the BEVs. If PV_{share} increases but EV_{share} does not, the NLVR slightly decreases, since the ability to store the PV power over-production is limited by the smaller EV fleet size. In both the V1G and V2G cases, about 2.5 EVs per installed PV system are needed to achieve the best NLVR in the present case study.

5. Impact analysis

In this section, the impact of smart charging is analysed based on a number of key performance indicators (KPIs) defined in Section 5.1. Results are compared w.r.t. of energy self-sufficiency (Section 5.2), battery degradation (Section 5.3), and economic profitability for the EV owners (Section 5.4).

5.1. KPIs description

The KPIs used in the rest of this paper to evaluate the impact of the proposed smart EV charging algorithm are defined below.

- *Self Sufficiency:* this is defined as the ratio between the yearly PV energy consumed by both EVs and other loads and the total yearly electric energy demand of the same user. A variant of this KPI only considers the EV load at the denominator. Further details are provided in Section 5.2.
- *Yearly* CO_2 *Emissions:* this is estimated as the product of the total amount of electric energy drawn from the grid and a coefficient k_{CO_2} representing the average amount of CO_2 emissions produced by consuming each kWh of energy coming from the grid. Such a coefficient depends on the energy mix of a country (e.g. k_{CO_2} = 241 g/kWh in Italy). Further details are provided in Section 5.2.

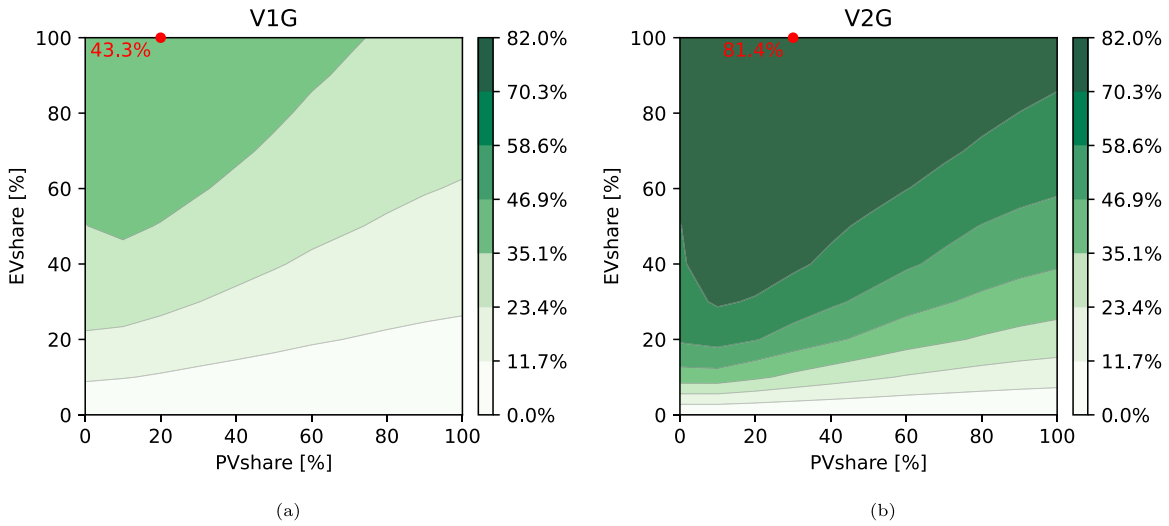

Fig. 4. Contour lines of the Net-Load Variance Reduction (NLVR) [%] at the substation w.r.t. the case when no smart charging is used for increasing values of PV_{share} and EV_{share}. In Fig. 4(a), a V1G optimisation is performed, whereas in Fig. 4(b) the proposed V2G optimal smart EV charging is applied.

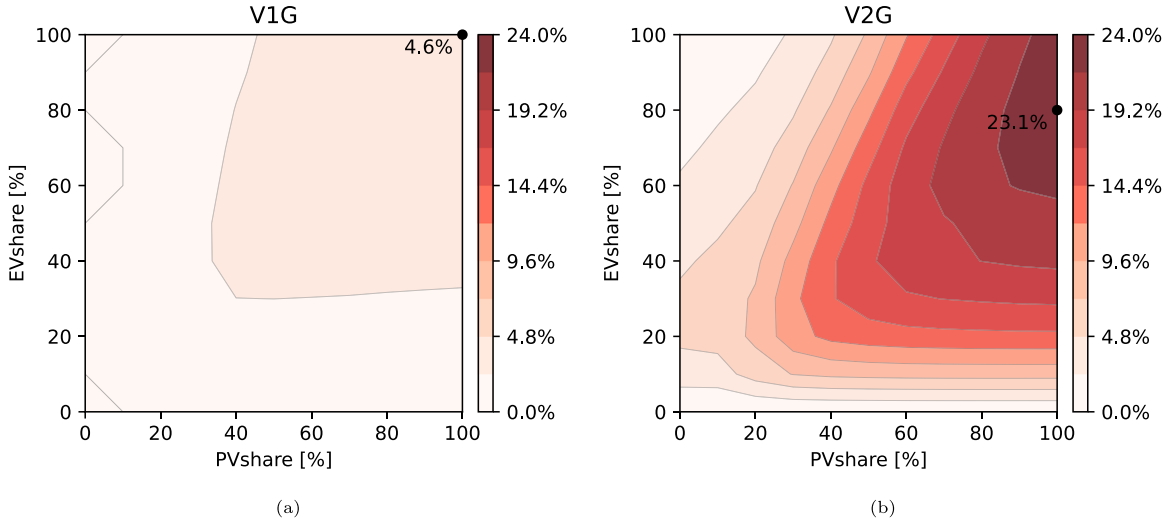

Fig. 5. Self-sufficiency (SU) increase for the total load in V1G mode 5(a) and V2G mode 5(b), respectively. SU is defined as the share of the total load covered by PV production.

- *Battery Degradation:* this is estimated by computing the relative variation in the state-of-health (SOH) of the EV batteries. This value requires to sum the contributions of the calendar and cycling battery ageing components, which are defined in greater detail in Section 5.3.
- *Economic Savings:* computed as the difference between the yearly cash flow when either the V1G or the V2G policy is applied and the baseline cash flow when charging is uncontrolled. This difference is then normalised by the baseline. The cash flows include the energy purchase and selling contributions, the battery degradation costs, and the costs to purchase and maintain an EV charging station. More details are presented in Section 5.4.

5.2. Self sufficiency and CO_2 emissions

Smart EV charging not only contributes to stabilising the grid, but also tends to improve the exploitation of distributed generators. Therefore, two very important performance metrics are analysed in the rest of this Section, i.e., the increase of the district-level energy self-sufficiency rate ΔSU, and the increase of the self-sufficiency rate ΔSU_{EV} for EV charging only, both w.r.t. the baseline case of UC EV charging.

Usually, the self-sufficiency (SU) is defined as the share of the total users' yearly electrical energy demand (due to both residential loads and EV charging, if present) which is either directly covered by a local PV generator, or by the energy buffered in the BEVs in V2G charging mode. The SU_{EV} rate instead is the ratio between the amount of PV energy used, directly or indirectly, to charge the EVs and the total EV energy consumption. Of course, the higher the values of these parameters, the lower the carbon footprint of the electrical distribution system and of the EV fleet, respectively. The contour lines of the absolute increments of ΔSU and ΔSU_{EV} obtained with both the V1G and the proposed V2G smart EV charging approaches w.r.t. the UC scenario are plotted in Figs. 5 and 6, respectively, as a function of both PV_{share} and EV_{share}.

Sizeable annual increases up to 23% are visible in Fig. 5 whenever the EVs are charged with the V2G-based policy. A large difference can be noticed between the two scenarios of Fig. 5. In V2G charging mode, the ΔSU peak value (of about 23%), reached when $PV_{share} = 100\%$ and $EV_{share} = 80\%$, is higher than the 4.6% reached in V1G mode. Such a large difference between the peak values can be explained by the fact that V1G is a "limited" form of V2G, as the batteries cannot be emptied during the night to absorb the PV energy during the day.

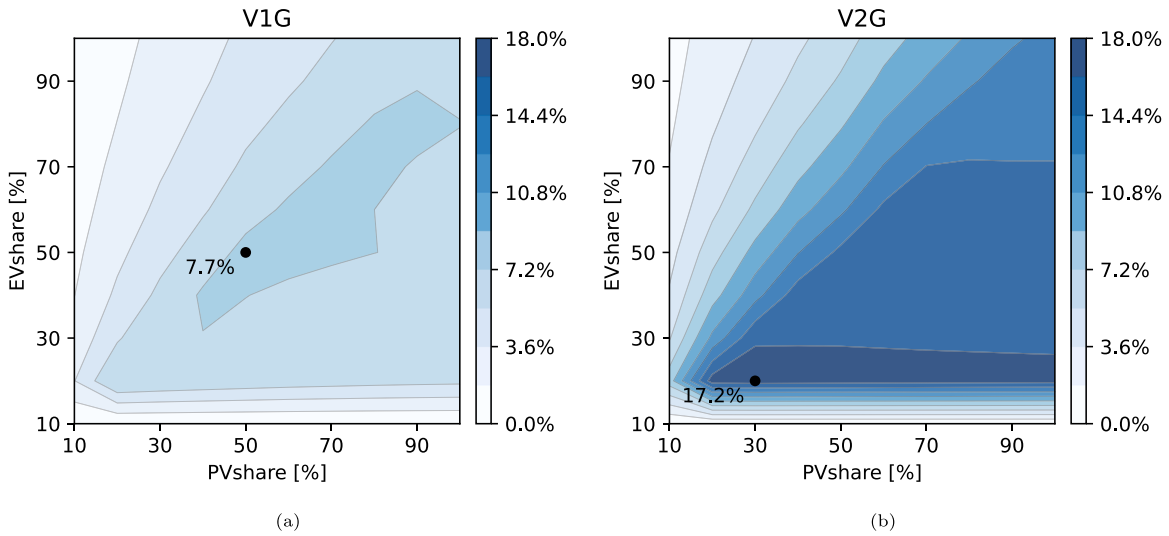

Fig. 6. Self-sufficiency (SU) increase for the EV load only in V1G mode 6(a) and V2G mode 6(b), respectively. SU is defined as the share of the total load covered by PV production.

Quite importantly, the EV_{share}/PV_{share} ratio for which the best ΔSU values are achieved is higher than the value that maximises the NLVR. This means that a better exploitation of PV energy may cause unwanted reverse power flow fluctuations over the distribution systems as well as at the substation transformer, due to the higher installed PV capacities. Considering that, for every kWh of electrical energy consumed in Italy, 241 g of CO_2 are emitted,[8] a self-sufficiency rate increase by about 23% may reduce the yearly CO_2 emissions in the district under study by 98 tCO2/year in the V2G scenario, and 28 tCO2/year in the V1G one.

Recalling that an ICV usually emits around 4.6 tCO2/year,[9] besides the inherent lower emissions of EVs compared to the those of an internal combustion vehicle (ICV), the application of the adopted V2G smart charging policy alone can save the emissions of 21 ICVs.

As far as the ΔSU_{EV} trend is concerned, the contour lines in Fig. 6 show that the ΔSU_{EV} values are rather stable when the ratio EV_{share}/PV_{share} is approximately constant. In the V1G case, the maximum increment of ΔSU_{EV} (between 7% and 8%, is achieved when $EV_{share}/PV_{share} \approx 1$ and half of the users installed a PV system. If the V2G smart EV charging policy is applied instead, the ΔSU_{EV} increments may be more than twice larger (up to 17.2%). However, the benefits of smart EV charging tend to saturate when the PV overproduction becomes excessive. Once more, these results are not surprising, because the objective of the optimisation was not to increase ΔSU_{EV}, but rather to minimise the NLV.

5.3. Battery degradation

The benefit of applying the V2G approach comes at the cost of a faster battery degradation, due to the higher number of charge/discharge cycles.

Following the methodology shown in [42] and further validated in [43], it is possible to quantify both the loss of capacity due to pure ageing (referred to as "calendar" contribution in the following) and the wear due to the number of charge/discharge cycles (namely, the "cycling" contribution). Based on the definitions above, if C_j denotes the nominal battery capacity of the $j-$th EV, the relative capacity reduction at time τ) results from the sum of two contributions, i.e. $\Delta SOH_j(\tau) = \frac{\Delta C_j^{CAL}}{C_j}(\tau) + \frac{\Delta C_j^{CYC}}{C_j}(\tau)$, where SOH is the State-of-health of the battery, representing the amount of useable battery capacity over the nominal one. In the previous equation, as reported in [44]:

$$\frac{\Delta C_j^{CAL}}{C_j}(\tau) = \frac{1}{2}\int_0^{\tau} \frac{f_j(t)}{\sqrt{t}} \cdot e^{-\frac{E_a}{R \cdot T_{b_j}(t)}} \cdot dt \tag{7}$$

is the relative capacity decrease due to the calendar time, which depends on:

- a time-varying factor $f_j(t)$ which is a function of the SOC of the $j-$th battery. This is derived experimentally and it usually varies between about 300 $h^{-1/2}$ (when the SOC is 0%) to about 1500 $h^{-1/2}$ (when the SOC is 100%) [45], i.e., it increases the calendar degradation if the battery is kept at high SOC values;
- E_a = 24500 J/mol, i.e., the activation energy of the battery chemical reaction [46];
- $R = 8.314\ \frac{\text{J}}{\text{mol}\cdot\text{K}}$, that is the universal gas constant;
- $T_{b_j}(t)$, i.e., the absolute battery pack temperature, assuming that the average temperature difference between the battery and the outdoor air temperature is around 3–4 °C [42].

On the other hand, the relative capacity decrease due to the number of charging–discharging cycles is given by [42]

$$\frac{\Delta C_j^{CYC}}{C_j}(\tau) = s_j \int_0^{\tau} B_1(t) \cdot e^{B_2(t)} \cdot |I_j(t)| \cdot dt \tag{8}$$

with $B_1(t) = a \cdot T_b(t)^2 + b \cdot T_b(t) + c$

and $B_2(t) = \left[d \cdot T_{b_j}(t) + e\right] \cdot \rho(t)$

where:

- $I_j(t)$ is the actual charging/discharging current of the $j-$th battery at time t;
- $a = 8.58 \cdot 10^{-6}\ \text{A}^{-1}\,\text{h}^{-1}\,\text{K}^{-2}$, $b = -5.1 \cdot 10^{-3}\ \text{A}^{-1}\,\text{h}^{-1}\,\text{K}^{-1}$, $c = 0.7589\ \text{A}\,\text{h}^{-1}$, $d = -6.7 \cdot 10^{-3}\ \text{h}\,\text{K}^{-1}$, $e = 2.344$ h, are empirical coefficients derived for a battery with a capacity of 1.5 Ah [46].
- $s_j = 1.5 \cdot V_{n_j}/C_j$ is a scaling corrective factor that keeps into account that the empirical coefficients a, b and c were estimated for a battery with capacity 1.5 Ah, while the battery capacity of the $j-$th EV is C_j. The nominal battery voltage V_{n_j} (usually 200–400 V) is assumed to be constant for each EV.
- $\rho_j(t)$ is the charging/discharging rate of the battery under study, adjusted to cause the same amount of degradation that was observed in a 1.5 Ah battery [42].

[8] EEA Greenhouse gas emission intensity of electricity generation, 2022, https://www.eea.europa.eu/ims/greenhouse-gas-emission-intensity-of-1

[9] Tailpipe Greenhouse Gases Emissions From A Typical Passenger Vehicle, Environmental Protection Agency US, https://nepis.epa.gov/Exe/ZyPDF.cgi?Dockey=P1017FP5.pdf

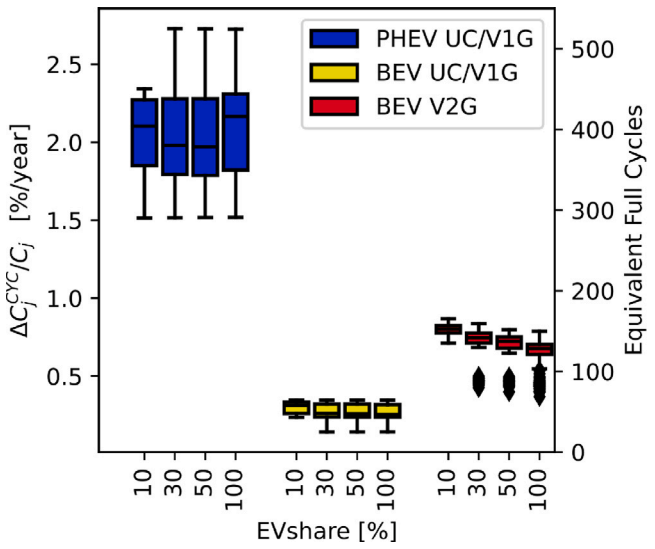

Fig. 7. Box-and-whiskers plot of the average relative capacity loss per year due to cyclic charging/discharging of PHEV and BEV batteries when different charging policies (i.e., uncoordinated, V1G and V2G) are adopted. On the right axis, the equivalent number of battery charging/discharging cycles per year are also shown.

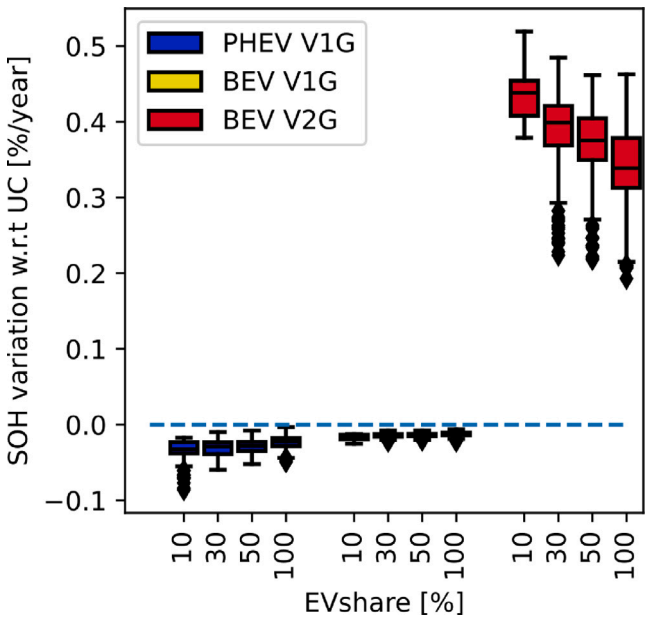

Fig. 8. Box-and-whiskers plot of the differences between the average SOH reduction per year in V1G or V2G mode and the corresponding baseline yearly SOH reduction values when the standard uncontrolled EV charging is applied.

Considering that the battery degradation is a very slow process and that the time quantities in the computation of empirical coefficients in (8) are expressed in h or h^{-1}, τ will be expressed in h as well in the rest of this Section. The dynamic degradation model of the EV battery capacity based on Eqs. (7)–(8) was implemented in Simulink, and simulations were run over multiple years.

The impact of the UC, V1G and V2G charging policy on the calendar ageing term (7) is minor and it is mainly due to the different profiles of $f_j(t)$. In particular, since the V1G and V2G techniques tend to charge the battery more slowly, the actual SOC values (particularly those of the PHEVs, whose batteries are depleted more frequently) are kept at lower SOC levels (on average) than $SOC^{\max}$ for longer time intervals. As a result, the average loss of capacity per year due to calendar ageing (computed over a time horizon of 10 years, i.e., the average vehicle lifetime in the EU [47]) is generally between 1.2%–1.3%/year in UC mode, while the actual degradation in V1G or V2G mode tends to decrease by about 0.1–0.2%/year. Note that larger variations (±0.2%/year) can be noticed in the case of PHEVs, due to their lower battery size.

Fig. 7 shows the range of both the average relative capacity loss per year due to cyclic charging/discharging based on (8) (y-axis on the left), as well as the corresponding equivalent yearly number of full charging/discharging cycles (y-axis on the right) for increasing EV_{share} values, and when different charging policies are adopted. Note that no specific values of PV_{share} are chosen in this case, since we verified that the battery capacity reduction is not significantly affected by the PV penetration level. The relative capacity reductions of PHEVs and BEVs are presented separately since the battery size greatly impacts both the mean value and the standard deviation of the capacity reduction. However, the results obtained with UC or V1G charging are aggregated because the V1G approach only schedules the charging sessions at a later time and/or modulates the amount of charging power. It does not, instead, influence the yearly number of equivalent full cycles, and it is quite independent of the value of EV_{share}. Indeed, in the case of UC or V1G charging, the PHEVs are fully charged/discharged about 400 ± 100 times per year (i.e. once every 0.75–1.25 days), while the full charging/discharging cycles of BEVs range between about 50–75 times per year (i.e., once every 5–7 days). This is in line with the total consumption assuming that each EV owner travels 11300 km/year on average, as explained in Section 4).

In the V2G charging mode, the battery capacity reduction of the BEVs is reported only, since the PHEVs were excluded from grid support to avoid excessive battery degradation, as explained in Section 4.4. It is clearly visible how the V2G policy quadruples the number of cycles for low EV_{share} values. Note that the V2G approach causes an increase in the number of cycles per BEV which is inversely proportional to EV_{share}. This happens because, the more the EVs available to smooth out the power profile at the transformer, the less each of them is going to be used, hence the lower equivalent cycles. Nonetheless, even when $EV_{share} = 100\%$, the number of charging/discharging cycles, as well as the related battery degradation, are almost doubled w.r.t. the V1G case.

Finally, the relative battery degradation data due to calendar ageing and charging/discharging cycles are added and used to plot Fig. 8, which shows the box-and-whiskers plot of the difference between the average yearly ΔSOH values of PHEVs and BEVs with and without smart charging. This final box-and-whisker plot reveals that the V1G charging scheme does not significantly affect battery degradation and the related lifetime. On the contrary, a slight improvement can be observed, due to the lower calendar ageing when the batteries are charged at a lower average SOC (i.e., more slowly). In the case of V2G charging instead, the ΔSOH increment for BEVs (which is in the order of a fraction of one percent unit per year) tends to shorten the battery lifetime by around 6 years, from an average value of 20 to 14 years. Note how 14 years is still higher than the average lifetime of an EV in the EU, meaning that the battery will, in most cases, not be replaced. That being said, the additional V2G SOH degradation diminishes as EV_{share} grows, because the grid support is provided by a higher number of EVs, thus reducing its impact on each.

5.4. An example of economic analysis

In this section, an example of economic analysis is presented to assess and compare the profitability of smart EV charging policies for the EV owners. The reported analysis relies on the two following basic assumptions:

i. The electric energy buying (retail) and selling (day-ahead) prices are based on the Italian market scenario in 2023.

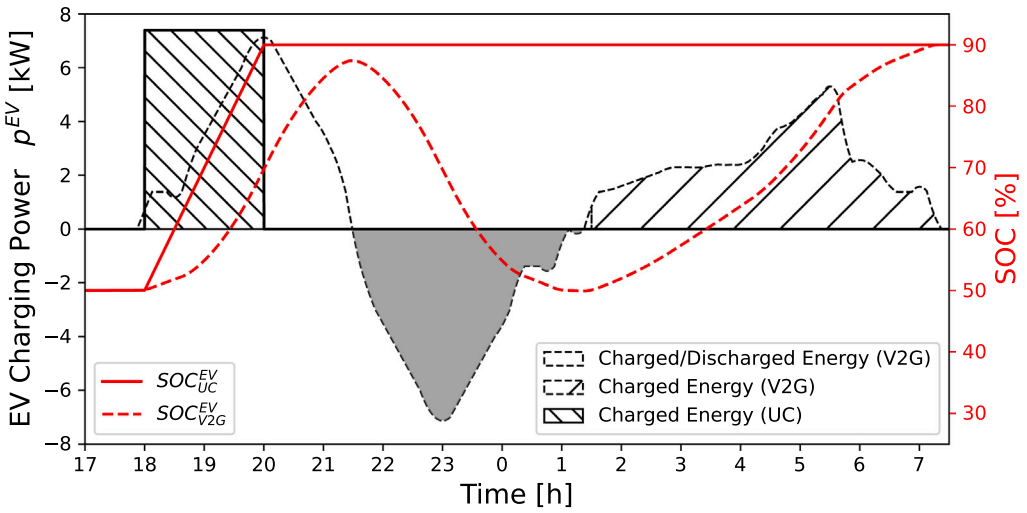

Fig. 9. Qualitative comparison between the UC BEV charging policy and the V2G one. The striped regions underlying the power profiles highlight the amount of energy bought by the user to reach $SOC^{\max}$. The equal white and grey areas represent the amount of energy that is first temporarily stored in the BEV battery (therefore, it is reimbursed by the Distribution System Operator — DSO) and then it is returned to the grid (in this case it is sold at the same price as the PV energy). The SOC profiles in the UC and V2G charging modes are also qualitatively shown for reference.

ii. The time horizon of the economic analysis is one year. However, since the EV batteries' degradation-related costs are spread over their entire lifetime, average yearly costs are included in the analysis.

Recalling the notation already adopted in Section 3, in the following, we will denote the average net power flow within the $t-$th time slot of the $n-$th user owning an EV as $p^{NET}_{j,t} = p^{L}_{j,t} + p^{EV}_{j,t} - p^{PV}_{j,t}$ for $j \in \mathcal{U}_{EV}$ and $t = 1, \dots, Y$, where $Y = 365 \cdot T$ is the number of 15-minute-long time slots in a year. Observe that, in the previous expression, the sequence of $p^{EV}_{j,t}$ values depends on the adopted EV charging policy (i.e., UC, V1G or V2G), whereas the sequence of $p^{PV}_{j,t}$ values is different from 0 for some t only if the $j-$th user is equipped with a local PV generator. If the time slot duration Δt is expressed in h (as in Section 5.3), and no flat additional compensation is offered by DSO for grid-support services (which is a conservative, but realistic assumption), then the actual yearly cash flow for the $j-$th user is given by

$$CF_j = \sum_{t=1}^{Y} \left[c^{buy}_t \max(p^{NET}_{j,t}, 0) + c^{sell}_t \min(p^{NET}_{j,t}, 0) \right] \Delta t + \overline{c}^{deg}_j + \overline{c}^{hw} \tag{9}$$

where:

- c^{buy}_t is the retail price of electricity at time t including system charges and taxes (e.g., about 0.32 €/kWh on average in Italy in 2023);
- c^{sell}_t is chosen as the pure hourly day-ahead market price (e.g., about 0.13 €/kWh on average in Italy in 2023);
- $\overline{c}^{deg}_j$ is the average cost per year due to battery degradation when a battery pack replacement is needed during the lifetime of the $j-$th EV. With this formulation, if $\overline{LT}_{EV}$ denotes the average lifetime of a vehicle (e.g., about 10 years in Europe [47]) and LT_j is the predicted battery lifetime of the $j-$th EV obtained from the battery degradation analysis, then $\overline{c}^{deg}_j = 0$ when $LT_j > \overline{LT}_{EV}$, and $\overline{c}^{deg}_j = \frac{c^{batt} C_j}{LT_j}$ otherwise. In the previous expression, c^{batt} is the battery cost per kWh (currently about 139 €/kWh[10]). Of course, the value of LT_j depends on both the battery size and the adopted charging/discharging policy, as explained in Section 5.3. To perform the current economic analysis, we assumed that the battery should be replaced when the average SOH variation exceeds 20% during the vehicle estimated lifetime (i.e., when $\overline{\Delta SOH}_j(\tau) \geq 20\%$ for $\tau < \overline{LT}_{EV}$ [48,49]).
- $\overline{c}^{hw}$ is the average yearly cost for purchasing and maintaining the EV charger, assuming that its lifetime is 15 years [50]. If, as explained in Section 4.2, the yearly consumption of a BEV is about 2.05 MWh on average, based on the cost model presented in [50], the overall cost of a unidirectional EV charging station (including operation and maintenance costs) is about 3075 €(i.e. $\overline{c}^{hw} = 205$ €/year). However, since the current hardware costs for purchasing a V2G charger are much higher [51], the $\overline{c}^{hw}$ value in the V2G case is about 273 €/year.

In (9), the first term is the yearly expense due to the actual energy consumption, while the second one (which is certainly negative) is the yearly economic revenue due to the amount of PV or EV power that is injected into the grid by the $j-$th user. Finally, the third term is the cost due to battery degradation.

It is worth emphasising that the simple economic model based on (9) is certainly not profitable for EV users when any V2G smart charging scheme (not just the proposed one) is applied. The reason is twofold. Firstly, the BEV battery lifetime in V2G mode decreases due to an increased number of cycles. Secondly, part of the energy stored in the EV battery is bought twice and sold once. Since in (9) the selling price is lower than the buying price, this economic model is inherently disadvantageous and unacceptable for a final user. Moreover, this is unfair considering that the user provides a service to the DSO.

To counteract these problems and make the V2G approach economically acceptable, some compensation is needed. This must be fair for the user and not too expensive for the DSO. In the following, a very simple and conservative compensation model is adopted, i.e., the EV owner is not charged for the extra amount of energy that is temporarily stored into the EV battery to be injected back in the power grid. In addition, the EV owner is remunerated by the DSO at the day-ahead market price c^{sell}_t when the energy is returned (as for the PV energy injection). In Fig. 9, the different hatched regions underlying the power charging profiles highlight the amount of energy that is bought by the user in UC or V2G mode to fully charge the BEV battery. Of course, the area of the striped regions in UC and V2G mode must be the same. The equal white and grey areas instead represent the amount of energy that is first temporarily stored in the BEV battery (and, therefore, reimbursed by the DSO) and then injected into the grid at the day-ahead market price. If such a compensation model is applied, the cash flow expression (9)

[10] Electric Vehicle Outlook 2023, BloombergNEF, https://about.bnef.com/electric-vehicle-outlook/

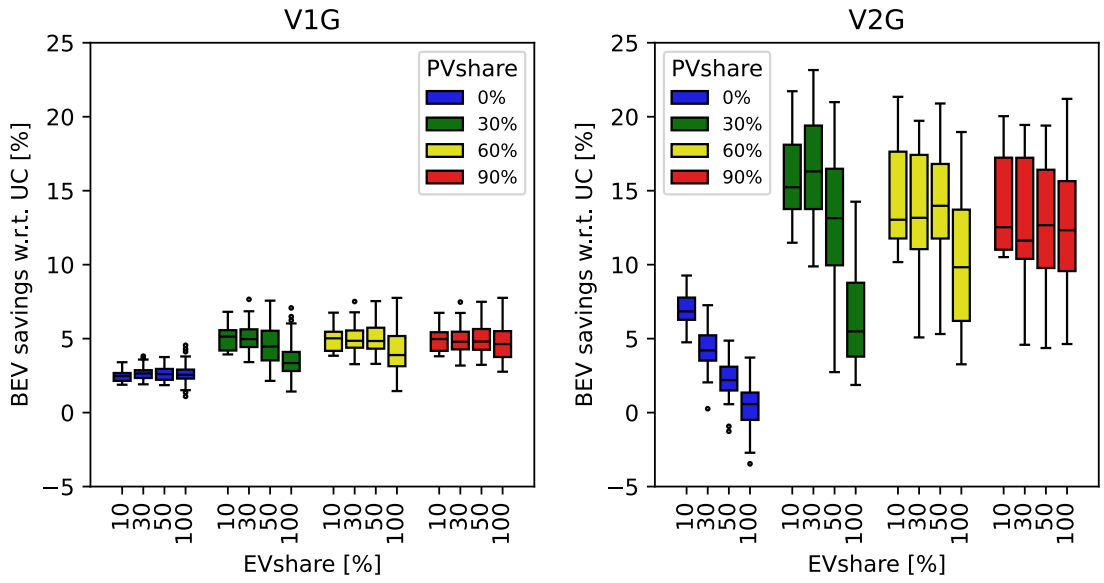

Fig. 10. Box-and-whisker plots of the relative yearly economic savings for the owners of BEVs charged in V1G mode 10(a) and V2G mode 10(b) w.r.t. the standard UC charging mode. The results refer to increasing EV and PV penetration levels.

changes as follows, i.e.,

$$CF_j^* = CF_j + \sum_{t=1}^{Y} c_t^{buy} \min(p_{j,t}^{EV}, 0) \cdot \Delta t \tag{10}$$

where the new term added to CF_j is either negative or null, as it represents the DSO reimbursement for the amount of extra energy that was temporarily stored in the battery and then returned to the DSO. The distribution of the possible relative yearly economic savings for BEV owners charging their vehicles in V1G or V2G mode w.r.t. the baseline UC charging are shown in Fig. 10, for increasing EV_{share} and PV_{share} values. The box-and-whiskers plots on the left and the right refer to the case of BEVs charged in V1G or V2G mode, respectively. The possible savings for the PHEVs owners (in V1G mode only) are not reported for the sake of brevity, but are quite comparable with those of BEV owners in V1G mode (commented below). In the present case study, the savings for BEV owners in V1G charging mode generally oscillate around 3%–5% (Fig. 10(a)), depending on whether a PV generator is available or not. In the former case, the savings are mainly due to the fact that PV energy is generally exploited better than in the standard UC charging mode. Note that, since the EV charging schedule in this paper is optimised to avoid power congestion at the substation transformer, the savings due to the usage of the PV energy are largely sub-optimal and tend to saturate, although with some fluctuations, as PV_{share} grows.

In V2G mode, the savings for the majority of BEV owners equipped with a local PV generator range between 10% and 20% (Fig. 10(b)). This is due to the joint effect of the DSO compensation and the better usage of the available PV energy. Indeed, the BEVs can discharge their battery to store some PV energy surplus, if present. One of the most important findings of this work is that the savings are not significantly affected by the battery degradation costs. Indeed, despite the higher V2G charging battery degradation confirmed by the results shown in Section 5.3, the need for battery replacement is unlikely during the EV lifetime. Furthermore, the average economic impact per year is minor.

6. Conclusions

In this article, we propose a centralised smart EV charging strategy with Vehicle-to-Grid (V2G) support, able to minimise the variance of the net-load power fluctuations at the substations' transformer of a distribution system in which a variable share of users are equipped with a residential PV generation unit. The daily EV charging schedules result from the solution of a Mixed-Integer Quadratically-Constrained Quadratic Programming (MIQCQP) problem, which is solved iteratively (i.e., considering one vehicle at a time) to ensure a good trade-off between sub-optimality of the results and scalability. If the integer decision variables of the problem are set to zero, the unidirectional V1G smart charging schedule for the same amount of EV charging stations and PV generators can be easily computed. The optimisation results over one year for increasing EV and PV penetration levels show that noticeable reductions of net load variance at the transformer can be obtained (up to about 43% in V1G mode and up to about 81% in V2G mode, respectively). The V2G smart charging mode also decreases the environmental impact, thanks to the increase of the PV self-sufficiency rate (between about 4% and 23% in the considered case study). The additional battery degradation for battery electric vehicles (BEVs) charged with the V2G approach is minor (i.e., between 0.2–0.5%/year on average) and it is mainly due to the higher number of charging/discharging cycles. However, for plug-in hybrid vehicles (PHEVs), the average degradation rate per year is generally 3–4 times higher than for BEVs. Therefore, this kind of EV should be excluded from V2G charging, as expected. From the economic standpoint, sizeable savings (between 10% and 20% on average) can be attained in V2G mode, if the BEV owners are also equipped with a PV generator and receive a reasonable compensation from the DSO for supporting the distribution system.

Future research directions should include (but not be limited to): the use of real EV charging and house load profiles; an economic analysis of the flexibility services procurement via controllable EVs for the DSOs; the development of multi-objective optimisation strategies aimed at minimising the NLV while maximising the economic benefits for users.

CRediT authorship contribution statement

M. Secchi: Writing – review & editing, Writing – original draft, Visualization, Validation, Software, Methodology, Formal analysis, Conceptualization. **D. Macii:** Writing – review & editing, Writing – original draft, Validation, Methodology, Conceptualization. **G. Barchi:** Writing – review & editing, Validation. **M. Marinelli:** Writing – review & editing, Validation.

Declaration of competing interest

The authors declare that they have no known competing financial interests or personal relationships that could have appeared to influence the work reported in this paper.

Acknowledgement

Part of this work was funded by the Horizon Europe project FLOW (Flexible energy systems Leveraging the Optimal integration of EVs deployment Wave), under grant agreement No. 101056730.

Data availability

Data will be made available on request.

References

[1] Secchi M, Ivanova A, Eichman J. Ev mobility diffusion and future perspectives in the eu: results from the flow project. In: 7th e-mobility power system integration symposium. (EMOB 2023), 2023, p. 1–8. http://dx.doi.org/10.1049/ICP.2023.2678.

[2] Bernard MR, Nicholas M, Wappelhorst S, Hall D. A review of the afir proposal: How much power output is needed for public charging infrastructure in the eu?. 2022, https://theicct.org/wp-content/uploads/2022/03/europe-ldv-review-of-afir-proposal-how-much-power-output-needed-for-public-charging-infrastructure-in-the-eu-mar22-2.pdf.

[3] Islam MR, Lu H, Hossain MJ, Li L. Optimal coordination of electric vehicles and distributed generators for voltage unbalance and neutral current compensation. IEEE Trans Ind Appl 2021;57:1069–80. http://dx.doi.org/10.1109/TIA.2020.3037275.

[4] Thingvad A, Andersen PB, Unterluggauer T, Træ holt C, Marinelli M. Electrification of personal vehicle travels in cities - quantifying the public charging demand. ETransportation 2021;9:100125. http://dx.doi.org/10.1016/J.ETRAN.2021.100125.

[5] Torquato R, Salles D, Pereira CO, Meira PCM, Freitas W. A comprehensive assessment of pv hosting capacity on low-voltage distribution systems. IEEE Trans Power Deliv 2018;33:1002–12. http://dx.doi.org/10.1109/TPWRD.2018.2798707.

[6] Hu J, Marinelli M, Coppo M, Zecchino A, Bindner HW. Coordinated voltage control of a decoupled three-phase on-load tap changer transformer and photovoltaic inverters for managing unbalanced networks. Electr Power Syst Res 2016;131:264–74. http://dx.doi.org/10.1016/J.EPSR.2015.10.025.

[7] Secchi M, Barchi G, Macii D, Petri D. Smart electric vehicles charging with centralised vehicle-to-grid capability for net-load variance minimisation under increasing ev and pv penetration levels. Sustain Energy, Grids Networks 2023;35:101120. http://dx.doi.org/10.1016/J.SEGAN.2023.101120.

[8] Tchagang A, Yoo Y. V2b/v2 g on energy cost and battery degradation under different driving scenarios, peak shaving, and frequency regulations. World Electr Veh J 2020 2020;11:14. http://dx.doi.org/10.3390/WEVJ11010014.

[9] Garruto R, Longo M, Yaï ci W, Foiadelli F. Connecting parking facilities to the electric grid: A vehicle-to-grid feasibility study in a railway station's car park. Energies 2020;13:3083. http://dx.doi.org/10.3390/EN13123083.

[10] Abdullah-Al-Nahid S, Khan TA, Taseen MA, Jamal T, Aziz T. A novel consumer-friendly electric vehicle charging scheme with vehicle to grid provision supported by genetic algorithm based optimization. J Energy Storage 2022;50:104655. http://dx.doi.org/10.1016/J.EST.2022.104655.

[11] Zhang L, Sun C, Cai G, Koh LH. Charging and discharging optimization strategy for electric vehicles considering elasticity demand response. ETransportation 2023;18:100262. http://dx.doi.org/10.1016/J.ETRAN.2023.100262.

[12] Jadoun VK, Sharma N, Jha P, Jayalakshmi NS, Malik H, Márquez FPG. Optimal scheduling of dynamic pricing based v2 g and g2v operation in microgrid using improved elephant herding optimization. Sustainability 2021;13:7551. http://dx.doi.org/10.3390/SU13147551.

[13] Huang P, Tu R, Zhang X, Han M, Sun Y, Hussain SA, et al. Investigation of electric vehicle smart charging characteristics on the power regulation performance in solar powered building communities and battery degradation in sweden. J Energy Storage 2022;56:105907. http://dx.doi.org/10.1016/J.EST.2022.105907.

[14] Li S, Gu C, Zeng X, Zhao P, Pei X, Cheng S. Vehicle-to-grid management for multi-time scale grid power balancing. Energy 2021;234:121201. http://dx.doi.org/10.1016/j.energy.2021.121201.

[15] Hussain A, Bui VH, Musilek P. Local demand management of charging stations using vehicle-to-vehicle service: A welfare maximization-based soft actor-critic model. ETransportation 2023;18:100280. http://dx.doi.org/10.1016/J.ETRAN.2023.100280.

[16] Park K, Moon I. Multi-agent deep reinforcement learning approach for ev charging scheduling in a smart grid. Appl Energy 2022;328:120111. http://dx.doi.org/10.1016/J.APENERGY.2022.120111.

[17] Shibl M, Ismail L, Massoud A. Electric vehicles charging management using machine learning considering fast charging and vehicle-to-grid operation. Energies 2021;14:6199. http://dx.doi.org/10.3390/EN14196199.

[18] Bartolini A, Comodi G, Salvi D, Østergaard PA. Renewables self-consumption potential in districts with high penetration of electric vehicles. Energy 2020;213:118653. http://dx.doi.org/10.1016/J.ENERGY.2020.118653.

[19] Heinisch V, Göransson L, Erlandsson R, Hodel H, Johnsson F, Odenberger M. Smart electric vehicle charging strategies for sectoral coupling in a city energy system. Appl Energy 2021;288:116640. http://dx.doi.org/10.1016/J.APENERGY.2021.116640.

[20] Fachrizal R, Munkhammar J. Improved photovoltaic self-consumption in residential buildings with distributed and centralized smart charging of electric vehicles. Energies 2020;13(5):1153. http://dx.doi.org/10.3390/en13051153.

[21] Fachrizal R, Qian K, Lindberg O, Shepero M, Adam R, Widén J, et al. Urban-scale energy matching optimization with smart ev charging and v2 g in a net-zero energy city powered by wind and solar energy. ETransportation 2024;20:100314. http://dx.doi.org/10.1016/J.ETRAN.2024.100314.

[22] Palmiotto F, Zhou Y, Forte G, Dicorato M, Trovato M, Cipcigan LM. A coordinated optimal programming scheme for an electric vehicle fleet in the residential sector. Sustain Energy, Grids Networks 2021;28:100550. http://dx.doi.org/10.1016/j.segan.2021.100550.

[23] Zhang S, Zhang S, Yeung LK, Yu JJ. Urban internet of electric vehicle parking system for vehicle-to-grid scheduling: Formulation and distributed algorithm. IEEE Trans Veh Technol 2023;1. http://dx.doi.org/10.1109/TVT.2023.3304718.

[24] Englberger S, Gamra KA, Tepe B, Schreiber M, Jossen A, Hesse H. Electric vehicle multi-use: Optimizing multiple value streams using mobile storage systems in a vehicle-to-grid context. Appl Energy 2021;304:117862. http://dx.doi.org/10.1016/J.APENERGY.2021.117862.

[25] Al-obaidi A, Farag HE. Optimal design of v2 g incentives and v2g-capable electric vehicles parking lots considering cost-benefit financial analysis and user participation. IEEE Trans Sustain Energy 2023;1. http://dx.doi.org/10.1109/TSTE.2023.3307633.

[26] Srithapon C, Månsson D. Predictive control and coordination for energy community flexibility with electric vehicles, heat pumps and thermal energy storage. Appl Energy 2023;347:121500. http://dx.doi.org/10.1016/J.APENERGY.2023.121500.

[27] Amry Y, Elbouchikhi E, Gall FL, Ghogho M, Hani SE. Optimal sizing and energy management strategy for ev workplace charging station considering pv and flywheel energy storage system. J Energy Storage 2023;62:106937. http://dx.doi.org/10.1016/J.EST.2023.106937.

[28] Cortés Borray AF, Merino J, Torres E, Garcés A, Mazón J, Borray AFC, et al. Centralised coordination of EVs charging and PV active power curtailment over multiple aggregators in low voltage networks. Sustain Energy, Grids Networks 2021;27:100470. http://dx.doi.org/10.1016/j.segan.2021.100470.

[29] Marano V, Onori S, Guezennec Y, Rizzoni G, Madella N. Lithium-ion batteries life estimation for plug-in hybrid electric vehicles. 5th IEEE Veh Power Propuls Conf VPPC ' 2009;09:536–43. http://dx.doi.org/10.1109/VPPC.2009.5289803.

[30] Hoke A, Brissette A, Maksimović D, Pratt A, Smith K. Electric vehicle charge optimization including effects of lithium-ion battery degradation. 2011 IEEE Veh Power Propuls Conf VPPC 2011 2011. http://dx.doi.org/10.1109/VPPC.2011.6043046.

[31] IEC. On and off-board equipment for charging evs with supply up to 1 kv ac and 1.5 kv dc. IEC 61851-1:2017. 2017.

[32] Shanno DF, Weil RL. 'Linear' programming with absolute-value functionals. Oper Res 1971;19(1):120–4, http://www.jstor.org/stable/168871.

[33] Misener R, Floudas CA. Global optimization of mixed-integer quadratically-constrained quadratic programs (MIQCQP) through piecewise-linear and edge-concave relaxations. Math Program 2012;136:155–82. http://dx.doi.org/10.1007/s10107-012-0555-6.

[34] ARERA. Arera's consultation document 449/2022 for electric mobility scenarios in italy. 2022, https://www.arera.it/fileadmin/allegati/docs/22/449-22.pdf.

[35] Hashim MS, Yong JY, Ramachandaramurthy VK, Tan KM, Mansor M, Tariq M. Priority-based vehicle-to-grid scheduling for minimization of power grid load variance. J Energy Storage 2021;39:102607. http://dx.doi.org/10.1016/j.est.2021.102607.

[36] Thingvad A, Calearo L, Andersen PB, Marinelli M. Empirical capacity measurements of electric vehicles subject to battery degradation from v2 g service. IEEE Trans Veh Technol 2021;70:7547–57. http://dx.doi.org/10.1109/TVT.2021.3093161.

[37] Thingvad A, Ziras C, Marinelli M. Economic value of electric vehicle reserve provision in the nordic countries under driving requirements and charger losses. J Energy Storage 2019;21:826–34. http://dx.doi.org/10.1016/J.EST.2018.12.018.

[38] González-Morán C, Arboleya P, Pilli V. Photovoltaic self consumption analysis in a European low voltage feeder. Electr Power Syst Res 2021;194(107087). http://dx.doi.org/10.1016/j.epsr.2021.107087.

[39] Pití A, Verticale G, Rottondi C, Capone A, Lo Schiavo L. The role of smart meters in enabling real-time energy services for households: the Italian case. Energies 2017;10(2).

[40] Secchi M, Barchi G, Moser D, Nassuato S, Pellizzari D, Costa A. Energy sharing control strategies: A benchmark analysis in a configurable italian demonstrator. 8th World Conf Photovolt Energy Convers 2022;1509–13. http://dx.doi.org/10.4229/WCPEC-82022-5CO.11.2.

[41] DTU Computing Center. DTU computing center resources. 2024, http://dx.doi.org/10.48714/DTU.HPC.0001.

[42] Calearo L, Thingvad A, Ziras C, Marinelli M. A methodology to model and validate electro-thermal-aging dynamics of electric vehicle battery packs. J Energy Storage 2022;55:105538. http://dx.doi.org/10.1016/J.EST.2022.105538.

[43] Marinelli M, Calearo L, Engelhardt J. A simplified electric vehicle battery degradation model validated with the nissan leaf e-plus 62-kwh. In: Proceedings of 6th international electric vehicle technology conference, 2023 6th international electric vehicle technology conference, eVTeC. 2023, Conference date: 22-05-2023 Through 24-05-2023.

[44] Wang D, Coignard J, Zeng T, Zhang C, Saxena S. Quantifying electric vehicle battery degradation from driving vs, vehicle-to-grid services. J Power Sources 2016;332:193–203. http://dx.doi.org/10.1016/j.jpowsour.2016.09.116.

[45] Keil P, Schuster SF, Wilhelm J, Travi J, Hauser A, Karl RC, et al. Calendar aging of lithium-ion batteries. J Electrochem Soc 2016;163:A1872. http://dx.doi.org/10.1149/2.0411609JES.

[46] Wang J, Purewal J, Liu P, Hicks-Garner J, Soukazian S, Sherman E, et al. Degradation of lithium ion batteries employing graphite negatives and nickel–cobalt–manganese oxide spinel manganese oxide positives: Part 1, aging mechanisms and life estimation. J Power Sources 2014;269:937–48. http://dx.doi.org/10.1016/J.JPOWSOUR.2014.07.030.

[47] Acea. Vehicles in use europe report, february 2024. 2024, https://www.acea.auto/files/ACEA-Report-Vehicles-on-European-roads-.pdf.

[48] Gou B, Xu Y, Feng X. An ensemble learning-based data-driven method for online state-of-health estimation of lithium-ion batteries. IEEE Trans Transp Electrification 2021;7:422–36. http://dx.doi.org/10.1109/TTE.2020.3029295.

[49] Fan Z, Zi-xuan X, Ming-hu W. State of health estimation for li-ion battery using characteristic voltage intervals and genetic algorithm optimized back propagation neural network. J Energy Storage 2023;57:106277. http://dx.doi.org/10.1016/J.EST.2022.106277.

[50] Lanz L, Noll B, Schmidt TS, Steffen B. Comparing the levelized cost of electric vehicle charging options in europe. Nat Commun 2022;13. http://dx.doi.org/10.1038/S41467-022-32835-7.

[51] Thune P, Macheca D, Zepter JM, Marinelli M, Malkova A, Høj S. Business cases and technological trends in vehicle-to-grid applications for residential users and fleet vehicles — welcome to DTU research database. 2024, https://orbit.dtu.dk/en/activities/business-cases-and-technological-trends-in-vehicle-to-grid-applic.